

Fabrication and stability of dual Pickering double emulsions stabilized with food-grade particles

Original

Fabrication and stability of dual Pickering double emulsions stabilized with food-grade particles / Tenorio-Garcia, Elizabeth; Rappolt, Michael; Sadeghpour, Amin; Simone, Elena; Sarkar, Anwasha. - In: FOOD HYDROCOLLOIDS. - ISSN 0268-005X. - 156:(2024), pp. 1-12. [10.1016/j.foodhyd.2024.110327]

Availability:

This version is available at: 11583/2991495 since: 2024-08-05T09:08:08Z

Publisher:

Elsevier

Published

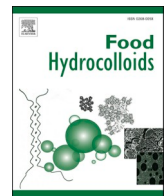
DOI:10.1016/j.foodhyd.2024.110327

Terms of use:

This article is made available under terms and conditions as specified in the corresponding bibliographic description in the repository

Publisher copyright

(Article begins on next page)



Fabrication and stability of dual Pickering double emulsions stabilized with food-grade particles

Elizabeth Tenorio-Garcia^a, Michael Rappolt^a, Amin Sadeghpour^a, Elena Simone^{a,b}, Anwasha Sarkar^{a,*}

^a Food Colloids and Bioprocessing Group, School of Food Science and Nutrition, University of Leeds, Leeds, LS2 9JT, UK

^b Department of Applied Science and Technology (DISAT), Politecnico di Torino, Torino, 10129, Italy

ARTICLE INFO

Keywords:

W/O/W emulsion
Microgels
Cocoa butter crystal
Stability
Whey protein
Double emulsion

ABSTRACT

The aim of this study was to create stable, dual Pickering-stabilized double emulsions (DEs) where both the internal and external droplets are stabilized by food grade particles. Water-in-oil (W/O) emulsions were stabilized by using cocoa butter-high oleic sunflower oil based oleogels (CBolg) and then W/O emulsion was used as the dispersed phase in water-in-oil-in-water (W/O/W) emulsions, latter stabilized by whey protein microgels (WPM). The capability of the CBolg (10 v/v% cocoa butter) to form W/O and subsequently a W/O/W emulsion was characterized using cross-polarized light microscopy, cryogenic scanning electron microscopy (cryo-SEM), confocal light microscopy (CLSM) and static light scattering. In addition, the characterization of the WPM's internal structure was evaluated by small angle X-ray scattering (SAXS). Results revealed dual Pickering stabilized W/O/W emulsions with a droplet size of 10 μm could be formed using whey protein microgel (WPM, 3–5 v/v%) as the Pickering stabilizer. Dynamic light scattering (DLS) analysis revealed WPM particles size averaging approximately 100 nm, with internal structures consisting of partially stretched protein strands with smaller compact subunits along the strand (partially folded proteins) was confirmed by SAXS analysis. The dual Pickering-stabilized DE droplets were stable over a month by formation a protective layer of WPM around the oil droplets, as observed in CLSM images, unlike the systems where the external phase was stabilized by non-microgelled whey protein, latter destabilized within hours. Such dual Pickering-stabilized DEs may offer new templates for designing healthy low-fat foods and for co-delivery of nutrients and active in multiple compartments.

1. Introduction

Double emulsions (DEs) are intricate dispersions of larger droplets containing smaller dispersed droplets of a different phase, with more susceptibility to destabilization as compared to simple emulsions (Tenorio-Garcia, Araiza-Calahorra, Simone, & Sarkar, 2022). Common categories of DE microstructures include water-in-oil-in-water (W/O/W) and oil-in-water-in-oil (O/W/O) emulsions (Cui, Zeng, Wang, & Zhang, 2017; Goibier, Pillement, Monteil, Faure, & Leal-Calderon, 2019; Wang, Hu, Zoghbi, Huang, & Xia, 2017). Their intricate compartmentalized microstructure endows DEs with promising application across various industries, serving as templates for encapsulation and delivery sensitive ingredients, masking taste, enhancing sensory attributes, and reducing fat content to lower calorie intake in food products. These multifaceted applications highlight the versatility of DEs in various sectors (Loffredi

& Alamprese, 2023; Tenorio-Garcia et al., 2022).

However, despite their potential, thermodynamic instability presents a major obstacle in industrial applications, even when stabilized with conventional surfactants such as polyglycerol polyricinoleate (PGPR) or E476 falls short in ensuring the required stability and shelf-life of the formulated product (Schuch, Kohler, & Schuchmann, 2013). The dual interfaces in DEs necessitate the used of different surfactants to stabilize the inner (W_1/O) emulsion and the secondary (O/W_2). While PGPR offers good stability to the W_1/O emulsion, its non-“clean-label” status poses limitations in food applications, prompting exploration into alternative stabilization methods like Pickering particles (Sarkar & Dickinson, 2020). Pickering particles, which are partially wetted at the liquid-liquid interface, manifest an almost irreversible adsorption process, provide a strong physical barrier to droplet coalescence. Pickering particles are attracting growing interests because of their potential to

* Corresponding author.

E-mail address: A.Sarkar@leeds.ac.uk (A. Sarkar).

<https://doi.org/10.1016/j.foodhyd.2024.110327>

Received 3 March 2024; Received in revised form 18 May 2024; Accepted 14 June 2024

Available online 20 June 2024

0268-005X/© 2024 The Authors. Published by Elsevier Ltd. This is an open access article under the CC BY license (<http://creativecommons.org/licenses/by/4.0/>).

form ultra-stable emulsions without relying on conventional surfactants. (Binks, 2002; Dekker et al., 2023).

The lack of edible particles to stabilize the water-oil interface has made the creation of Pickering DEs challenging, despite the promising opportunities in the field. Several particles have been proposed to stabilize W/O emulsions, including starch-based nanoparticles (Zhai et al., 2019), fat crystals (Ghosh & Rousseau, 2011; Ghosh, Tran, & Rousseau, 2011; Norton, Fryer, Parkinson, & Cox, 2009), polyphenol crystals (Zembyla, Lazidis, Murray, & Sarkar, 2019, 2020; Zembyla, Murray, Radford, & Sarkar, 2019), sunflower oleosomes (Karefyllakis, Jan van der Goot, & Nikiforidis, 2019), hydrothermally treated waste coffee particles (Gould, Garcia-Garcia, & Wolf, 2016), phytosterol particles (Lan et al., 2020). In addition, anhydrous milk fat (AMF), cocoa butter fat (CB) can be also be used to form stable W/O emulsion without further surfactants by manipulating fat crystal properties (Goibier, Pillement, Monteil, Faure, & Leal-Calderon, 2020; Tenorio-Garcia, Araiza-Calahorra, Rappolt, Simone, & Sarkar, 2023). However, many, if not most, of these systems have not been considered for the fabrication of Pickering DEs due to further instability of the second oil-water interface.

The external interface of W/O/W emulsions have been stabilized with a variety of Pickering particles, such as octenylsuccinate quinoa starch (Lin et al., 2020), hydroxyl propyl methyl cellulose, rutin hydrate (Spyropoulos, Duffus, Smith, & Norton, 2019), Zein particles (Jiang et al., 2021), kafirin particle (Xiao, Lu, & Huang, 2017), among others. However, challenges persist due to the poor wettability of these particles. Microgels have emerged as potential stabilizers for O/W simple emulsions (Destribats, Rouvet, Gehin-Delval, Schmitt, & Binks, 2014; Wu et al., 2015; Zhang, Holmes, Ettelaie, & Sarkar, 2020) and more recently in O/W/O DEs (Guan, Li, Jiang, Tse, & Ngai, 2023). They offer advantages as soft deformability and enhanced stability (Akgonullu et al., 2023; Chen et al., 2022; Dickinson, 2015).

The persistent stabilization issues encountered in simple emulsions, such as creaming, coalescence, flocculation, and Ostwald ripening of both water and oil droplets (e.g., W/O/W double emulsions), also extend to DEs, together with molecular diffusion phenomena (Nelis et al., 2019; Nollet, Laurichesse, Besse, Soubabère, & Schmitt, 2018). Several approaches have been used to mitigate diffusion, including 1) incorporating gelling agents into both the inner (W_1) and external water (W_2) phases, 2) incorporating fat crystals into the oil phase to gel the oil phase, and 3) carefully balance osmotic pressure through the addition of osmotic regulators such as glucose (Herzi & Essafi, 2019; Nelis et al., 2019). Fat crystals have been used to control diffusion from the dispersed phase, as the shell of crystals forming at the interface and/or the network limit diffusive transfer of molecules (Goibier et al., 2020; Liu et al., 2020; Nelis et al., 2019). However, limited studies have been performed on dual Pickering particles to stabilize DEs without the use of surfactants.

This study aims to evaluate the processability and stability of DEs stabilized solely by Pickering particles, utilizing natural compounds to avoid traditional surfactants like PGPR in the primary emulsion. To achieve this, a combination of cocoa butter (CB) fat crystals and whey protein microgel (WPM) particles were used to stabilize both internal and external droplets of the DEs, respectively. A comprehensive screening of different volume fraction of external Pickering particles composition (WPM) and processing parameters was conducted to engineer the most stable DE system. The dual Pickering DEs were compared with single Pickering DEs where the external droplets were stabilized by non-microgelled whey protein isolate (WPI) as a protein stabilization. The outcomes from this study will inform future development of innovative, stable, multicompartments, food systems, offering solutions to reduce fat content or effectively co-encapsulate water-soluble and oil-soluble components simultaneously, to enable the fabrication of the next generation of healthier and sustainable food structures.

2. Materials and methods

2.1. Materials

Refined, bleached, and deodorized cocoa butter (CB) and high oleic sunflower oil (HOSO) were obtained from Cargill (UK). The typical composition of the fatty acids presents in CB was 36% stearic acid, 34% oleic acid, 26% palmitic acid, 2.7% linoleic acid, and 0.9% arachidic acid by weight [8]. Meanwhile, HOSO typically contained 86% oleic acid, 5% stearic acid, 3% linoleic acid, 3% palmitic acid, 1.5% behenic acid, and 0.7% arachidic acid by weight [8]. Sodium phosphate monobasic monohydrate, sodium phosphate dibasic anhydrous, and hydroxyl chloride were purchased from Thermo Fisher Scientific Loughborough, UK. Sodium azide (0.02%) was obtained from Sigma Aldrich (USA) and used as an antibacterial agent. Whey protein isolate powder (WPI) containing $\geq 90\%$ protein was kindly donated by Fonterra Limited (Auckland, New Zealand). The phosphate buffer used to prepare the whey protein microgel (WPM) was Milli-Q water (water purified to a resistivity of $18 \text{ M}\Omega\cdot\text{cm}$ by Milli-Q apparatus, Millipore Corp., Bedford, MA, USA).

2.2. Preparation of Pickering particles

The stabilization of the primary emulsion (W/O) was achieved using a cocoa butter-based oleogel (CBolgs). In brief, CB and HOSO were blended at 55°C for 30 min to produce a 10% CB mixture. Controlled cooling lead to the formation of the $\beta(V)$ crystal structure in the CBolg (Tenorio-Garcia et al., 2023). Once the crystallization reached equilibrium, the temperature was adjusted to 20°C , crucial for emulsion stability due to CBolgs' low melting point (23°C) (Metilli et al., 2021; Tenorio-Garcia et al., 2023).

Pickering stabilization of the secondary emulsion in dual Pickering-stabilized DEs was achieved using whey protein microgel particles (WPM). An aqueous dispersion of 10 wt% of WPI was dissolved in 20 mM phosphate buffer during 2 h, allowing complete dissolution of the powder (Sarkar, Kanti, Gulotta, Murray, & Zhang, 2017). This solution was heated at 90°C for 30 min, cooled down at room temperature for 15 min and storage at 4°C overnight to form a hydrogel. A 5.0 wt% protein-containing hydrogel was broken into microgel fragments during 1 min using a hand blender (HB724, Kenwood, UK). The resulting dispersion was passed twice through a high-pressure homogenizer at 250 bar (Panda Plus, GEA Niro Soave, Parma, Italy). The resulting WPM particles containing 5.0 wt% protein in the dispersion were used to stabilize the secondary emulsion of the W/O/W DEs.

2.3. Wettability

The hydrophilic/hydrophobic character of the CBolg crystals was assessed by measuring the static water contact angle at 25°C using a OCA25 drop-shape tensiometer (DataPhysics Instruments, Germany) fitted with a microsyringe and a high-speed camera. Thin solidified films of the CBolg were prepared by melting the CB at 55°C and CBolgs were prepared with HOSO at two different concentrations: 10% and 20% (w/w) and were left on a flat surface until solidified. Static contact angles were measured using the sessile drop method. Water droplets ($3 \mu\text{L}$) were produced using a straight needle of 0.52 mm outer diameter and 0.26 mm internal diameter, to form a sessile drop onto the solidified CBolg surface. A video camera was used to record the droplet behavior. The droplet contour was fitted using the SCA software, and the static water contact angle was measured.

2.4. Fabrication of double emulsions

The continuous phase of the primary emulsion (W_1/O) consisted solely of CBolgs without surfactant addition, maintaining a water volume fraction of 30/70 throughout all the experiments. The dispersed

phase, phosphate buffer (20 mM at pH 7.0), was precooled to 4 °C in an ice bath to ensure a processing temperature of 21 °C during emulsification. Sodium azide was incorporated into the formulation at a concentration of 0.02 wt% to control microbial growth. Emulsions were prepared by mixing the cold-water phase with the CBolgs and emulsifying with *n* utilizing a rotor-stator emulsifier (Ultra-Turrax S25N-18G, IKA, Staufen) at 24,000 rpm for 40 s within a temperature-controlled vessel set at 20 °C to match the temperature for crystal formation (10 v/v% CB).

The resulting primary emulsion (W_1/O) was used as the dispersed phase to form the secondary O/W_2 emulsion, resulting in a $W_1/O/W_2$ double emulsion (see Fig. 1). The water volume fraction of the (W_1/O)/ W_2 emulsion was maintained at 20/80 ratio (6/14/80 final ratio). Once the primary emulsion was formed, it was weighted and added to the continuous phase containing either WPI to form single Pickering double emulsion or WPM to create dual Pickering double emulsions. The name “dual” is used here to indicate the presence of Pickering particles *i.e.* CBolgs in the W_1/O and WPM in the O/W_2 phase. The DEs were made in the jacketed vessel, maintaining the working temperature (20 °C) of the W_1/O emulsion, and emulsifying with the secondary water phase in a rotor-stator emulsifier (Ultra-Turrax S25N-18G, IKA, Staufen) at 9,400 and 11,000 rpm. Finally, the DEs were stored at a controlled temperature of 21 °C.

2.5. Optimization of formulation and manufacturing process

Following the formation of the DE, we evaluated the stability provided by WPI or WPM, along with the effects of various formulations and processing parameters. An initial experiment with WPI-based DEs were made using three different concentrations of WPI solutions (5.0–15.0 w/v%). For the WPM, we used a 2^5 factorial design to test the stability of the DEs stabilized with WPM, with the two factors under consideration being (a) WPM concentration (3.0 and 5.0 v/v%) and (b) time (assessed every 7 days over a span of 4 weeks). To quantitatively assess stability, we looked at changes in the DE microstructures and the distribution of oil droplet size using optical microscopy. For this set of experiments the homogenization speed used was 9,400 rpm. It is important to note that the processing conditions of the primary emulsion remained consistent across all experiments conducted. The second shearing step in the two-step emulsification process can influence the droplet size of DEs; therefore, two different homogenization velocities (9,400 rpm and 11,000 rpm) were evaluated to determine the optimal processing condition. Importantly, the effect of homogenization velocity was assessed solely on the most stable emulsion obtained from the previous experimental design.

2.6. Sizing of WPM Pickering particles and DEs

Dynamic light scattering (DLS) was used to measure the size

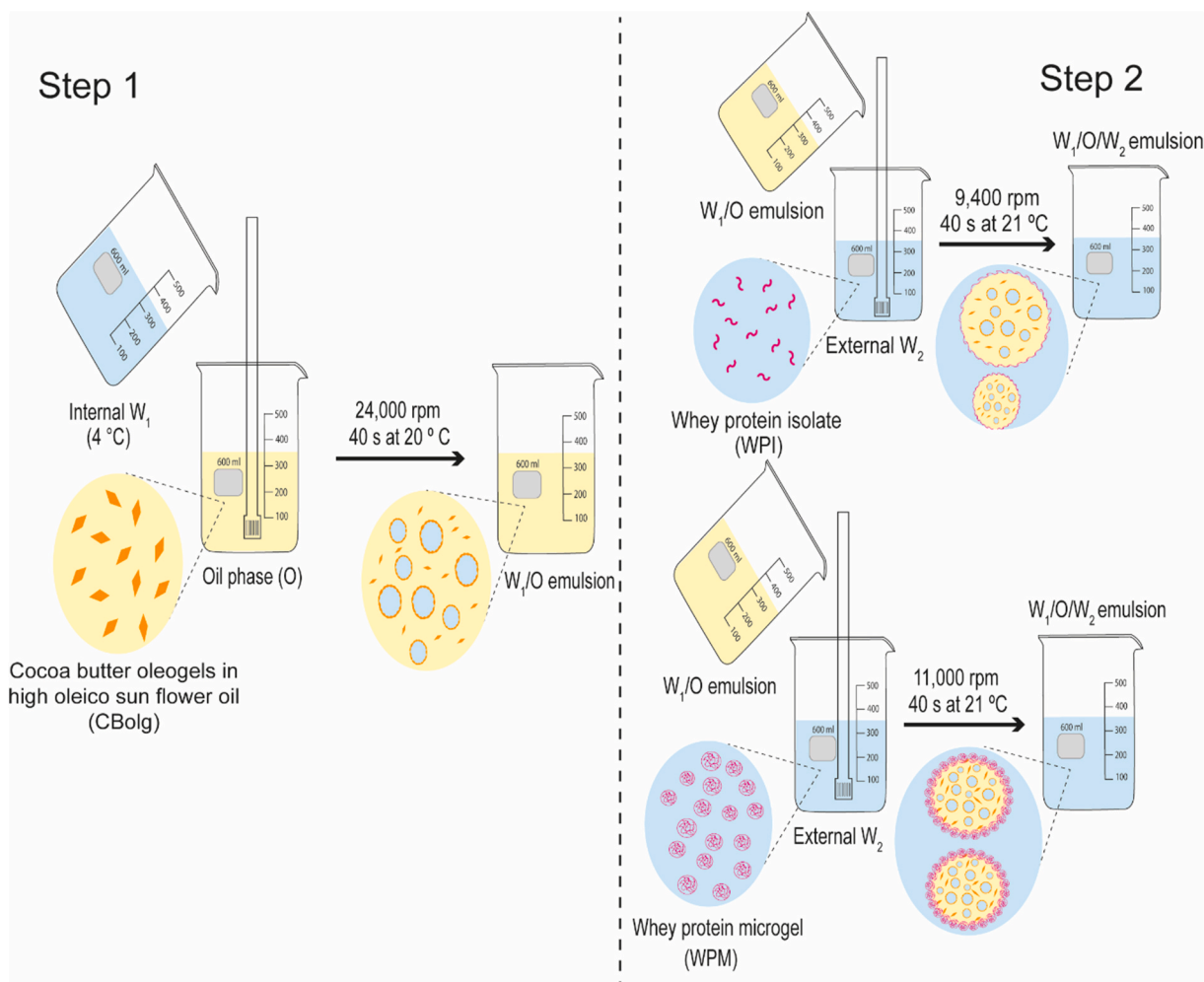


Fig. 1. Schematic illustration of the two step methodology of double emulsion (DE) process. The step one shows the processing of W_1/O emulsions made with the first Pickering particles *i.e.* cocoa butter-based oleogel crystals. The step two depicts the $W_1/O/W_2$ DE process using either a protein (whey protein isolate, WPI) or a Pickering stabilizer (whey protein microgels, WPM).

distribution of the WPM, while the droplet size distribution of the DEs was determined using static light scattering (SLS). Aqueous dispersions of WPM were measured at a temperature of 25 °C using a Zetasizer Nano-ZS (Malvern Instruments, Malvern UK) following a 100 × dilution in phosphate buffer (pH 7.0) at room temperature. The refractive index used for WPM was 1.5. Droplet size distribution of double emulsions, both before and after storage, was determined at room temperature (around 21 °C) using Malvern Mastersizer 3000 (Malvern Instruments Ltd, Malvern, Worcestershire, UK). The mean droplet size of the DEs was reported as volume mean diameter (d_{43}). The refractive index of the oil droplets was measured at 1.46, whilst the refractive index of the dispersant (external water) was 1.33.

2.7. ζ -potential measurements

The ζ -potential values of aqueous dispersions of the WPM were determined using a Zetasizer, Nano ZS series, Malvern Instruments, Worcestershire, UK. WPM was diluted to 0.01 v/v% particle concentration in phosphate buffer (pH 7.0) and added to a folded capillary cell (Model DTS 1070, Malvern Instruments Ltd., Worcestershire, UK).

2.8. Microscopy of the WPM and DEs

2.8.1. Optical microscopy (OM) and polarized light microscopy (PLM)

The morphology of the DEs was examined using optical and polarized microscopy techniques. To maintain a constant temperature of 21 °C, during the observation, the standard stage on the OM and PLM was replaced with a Cambridge Shearing system stage (CSS450, Linkam Scientific Instrument Ltd, UK). The CSS450 allows to control the desired temperature either heating the plate or cooling the plate with liquid nitrogen. A small amount of the DEs were placed in the quartz plate and the upper quartz plate was positioned with a micron accuracy at a distance from the bottom plate of 500 μm . One droplet of the diluted sample was placed in the quartz plate of the CSS450. The distance between the plates can be adjusted with the dedicated software, ranging from 0 to 2,500 μm . To visualize the crystals within the DE, a polarizer was integrated into the OM. The microscope was fitted with a Canon DSLR camera, and the digital images were acquired at 50 × magnification. Subsequently, the acquired images were processed using ImageJ software, version 1.52p (National Institute of Health, Bethesda, USA).

2.8.2. Confocal laser scanning microscopy (CLSM)

The morphology of the W/O/W DEs was characterized using a Zeiss LSM 880 inverted microscope (Carl Zeiss MicroImaging GmbH, Jena, Germany). Approximately, 10 μL of a mixture containing Nile Red (0.002 mg/mL in dimethyl sulfoxide, final concentration), Fast green (0.1 mg/mL in MilliQ water) and Nile blue (0.1 mg/mL in MilliQ water, final concentration) were added to 1 g of the DEs.

Emulsions were placed into a concave confocal microscope slide, covered with a glass coverslip, and observed 63 × oil immersion lens with pinhole maintained at 1 Air Unit to effectively filter out most of the light scattering. The wavelength used to excite Nile Red was 488 nm, for Nile Blue 625 nm, while Fast Green was excited at a wavelength of 633 nm. Three different dyes were employed in this study to identify various components within DEs. Nile red (NR) staining oil was helpful in confirming the existence of DEs by revealing water droplets encapsulated within the oil droplets, visually represented as red droplets-stained with discernible dark regions which correspond to the internal water. To highlight the presence of Pickering particles, two distinct dyes were utilized: Nile blue (NB) to identify CBolg crystals at the water-oil interface, and Fast green (FG) identify WPM at the oil-water interface, both appearing green due to their near-identical excitation wavelength. Noteworthy, that NB is a cationic dye with higher solubility in water than in oil. Despite its low oil solubility, NB has been employed in butter to achieve fluorescence contrast, given its solubility in the water phase allowing to distinguish between oil and fat crystals (Herrera & Hartel,

2001). Although, NB and NR have been used to stain the same fatty acid such as oleic acid in the literature (Boumelhem et al., 2021), it appears that NB exhibits a greater affinity for the chemical composition of the CB fat crystals as opposed to HOSO. Stained DEs were observed immediately after preparation and following one month of storage at 21 °C.

2.8.3. Cryogenic scanning electron microscopy (CryoSEM)

The morphology of W/O/W DEs containing a 30 wt% W₁/O emulsion stabilized with 10.0 v/v% CBolg crystals and the secondary emulsion containing 5.0 v/v% WPM, was acquired using a Helios G4 CX DualBeam scanning electron microscope (FEI, USA), coupled with a PP3010T Cryo-FIG/SEM system (Quorum Technologies, UK). The pre-cooled rivet holder was filled with a sample, which was quickly frozen with liquid nitrogen. The frozen sample was inserted in the preparation sample chamber and kept at -145 °C under vacuum ($<10^{-7}$ mbar), and then it was fractured with a cooled sharp knife to allow water sublimation at -90 °C. Then the sample was cooled again to -145 °C and sputtered with iridium (10 mA for 30 s). Finally, the sample was transferred inside the microscope chamber. Images were acquired at 2 kV accelerating voltage and 0.10 nA beam current.

2.8.4. Scanning electron microscopy (SEM)

The particle morphology of the WPM was imaged using Scanning electron microscope (Hitachi SU8230 FESEM (Hitachi, Japan). The WPM were mounted on specimen stubs and subjected to drying with hot air until the water was completely evaporated, a process lasting approximately 10 min. The dried WPM particles were coated with platinum (4 nm thickness) using a sputtering technique in a Leica ACE 600 sputter coater. The coated WPM were then analyzed at a magnification of 116,000× with an accelerating voltage of 2.0 mV.

2.9. Small-angle X-ray scattering (SAXS)

SAXS measurements were performed on the WPI and WPM solutions with a SAXSpace instrument (Anton Paar GmbH, Austria). The instrument is equipped with a Cu anode ($\lambda = 0.154$ nm). The temperature was set to 20 °C, which is controlled by a TCstage 150 sample holder equipped with a Peltier element (Anton Paar, Austria). The SAXS measurements were performed at a sample-detector distance of 320 mm. The 1D scattering patterns were recorded with a Mythen microstrip X-ray detector (Dectris Ltd., Baden, Switzerland).

The samples were loaded into a quartz capillaries with an outside diameter of 1.5 mm (Capillary Tube Supplies Ltd., Cornwall, UK). The phosphate buffer, WPI and WPM were injected into quartz capillaries with a long syringe needle and were subsequently sealed with wax. The SAXSTreat software (Anton Paar GmbH, Graz, Austria) was used to set to zero the position of the primary beam in all the patterns. The recorded scattering patterns were normalized for their transmission by using the SAXSQuant software (Anton Paar GmbH, Graz, Austria). From the normalized WPI and WPM pattern, the empty capillary and buffer scattering signals were subtracted. A peak fit analysis was carried out in OriginPro 2019b, by using standard linear plots applying Guinier and Porod models (Glatter & Kratky, 1982; Guinier & Fournet, 1955), and hereby using least-squares fits to the appropriate models. Further, we followed the procedures used on combined Guinier-Porod models published by Hammouda (2010) in the interpretation of the whey protein microgel (WPM) dispersion scattering.

2.10. Statistics

All quantitative results are based on three measurements on triplicate samples ($n = 3 \times 3$) and data is represented as a mean and standard deviation. One way analysis of variance to the WPM experiments with followed Tukey's multiple comparisons tests was employed to determine significant differences ($p < 0.05$) using the software Minitab.

3. Results and discussion

3.1. Characteristics of single Pickering stabilization: fat crystals for internal phase and proteins for external phase of DEs

Our previous research (Tenorio-Garcia et al., 2023) demonstrated the stability of water-in-oil (W/O) emulsions solely stabilized by 15CBolg crystals, revealing no phase separation and minimal droplet size variation ($0.37\ \mu\text{m}$ – $1.2\ \mu\text{m}$) after seven months of storage at $23\ ^\circ\text{C}$. These CBolg crystals, in $\beta(\text{V})$ polymorph, adsorbed at the W/O interface and contributed to the formation of a crystalline network in the bulk phase, thereby enhancing stability. In the literature, it is reported that fat crystals often have certain degree of polarity. A water contact static angle value of 95° has been reported for tempered CB (Reinke, Hauf, Vieira, Heinrich, & Palzer, 2015). However, in presence of HOSO (90 % HOSO), the water contact angle of CBolg crystals decreases to $68.3^\circ \pm 3.76$ (Fig. S1). This suggest that the crystals increase its preference to wet the aqueous phase (Boode & Walstra, 1993) as an oleogel unlike the pure CB crystals. Additionally, Johansson, Bergenstahl, and Lundgren (1995) observed that a looser packing in α and β' crystals resulted in slightly polar surfaces. In our previous findings (Tenorio-Garcia et al., 2023), CBolgs exhibited a slightly lower triacylglycerol (TAG) packing density, as determined by small and wide angle X-ray scattering (SAXS and WAXS), suggesting HOSO TAG influencing the crystal's arrangement in CBolg crystals, potentially forming co-crystals. Therefore, HOSO may have influenced the wettability of CB allowing the CBolg crystals to

act as Pickering stabilizer of the water droplets.

The utilization of these CBolg crystal-stabilized emulsions in the context of DE raise questions regarding the ability of CBolg resisting the secondary homogenization shear and the secondary surfactant maintaining DE structural integrity during storage. Previous studies in simple emulsions have demonstrated that a higher solid fat content (SFC) increases the likelihood of coalescence, as more crystals protrude through the oil droplet (Boode, Walstra, & de Groot-Mostert, 1993). Therefore, a precise tuning of the SFC to ensure a correct balance between oleogel melting point and resistance to coalescence is essential for designing a DE system that can perform effectively and with a reasonable shelf life. As the SFC is a function of both temperature and CB content, we decided to use oleogels with 10 v/v% CB (10CBolg) for emulsions processed and stored at $21\ ^\circ\text{C}$ in this work. The SFC (0.76%) of this system is comparable with that of 15CBolg at $24\ ^\circ\text{C}$ (used in our previous work (Tenorio-Garcia et al., 2023)) but it was easier to handle without the need of complex heating or cooling systems.

Fig. 2a shows the microstructure and stability of DEs obtained using different concentrations of non-microgelled WPI. As evident from the micrograph on day 0, depicted in Fig. 2a, the CBolg crystals exhibit remarkable strength, withstanding the second shearing step. This is discernible by the presence of brownish-dark droplets, signifying the existence of considerable proportions of internal water droplets and therefore the resistance of the CBolg crystals to hold the water during the secondary shearing processing. The droplet size distribution of freshly prepared DEs for 5.0 w/w% WPI was bimodal, with the first peak

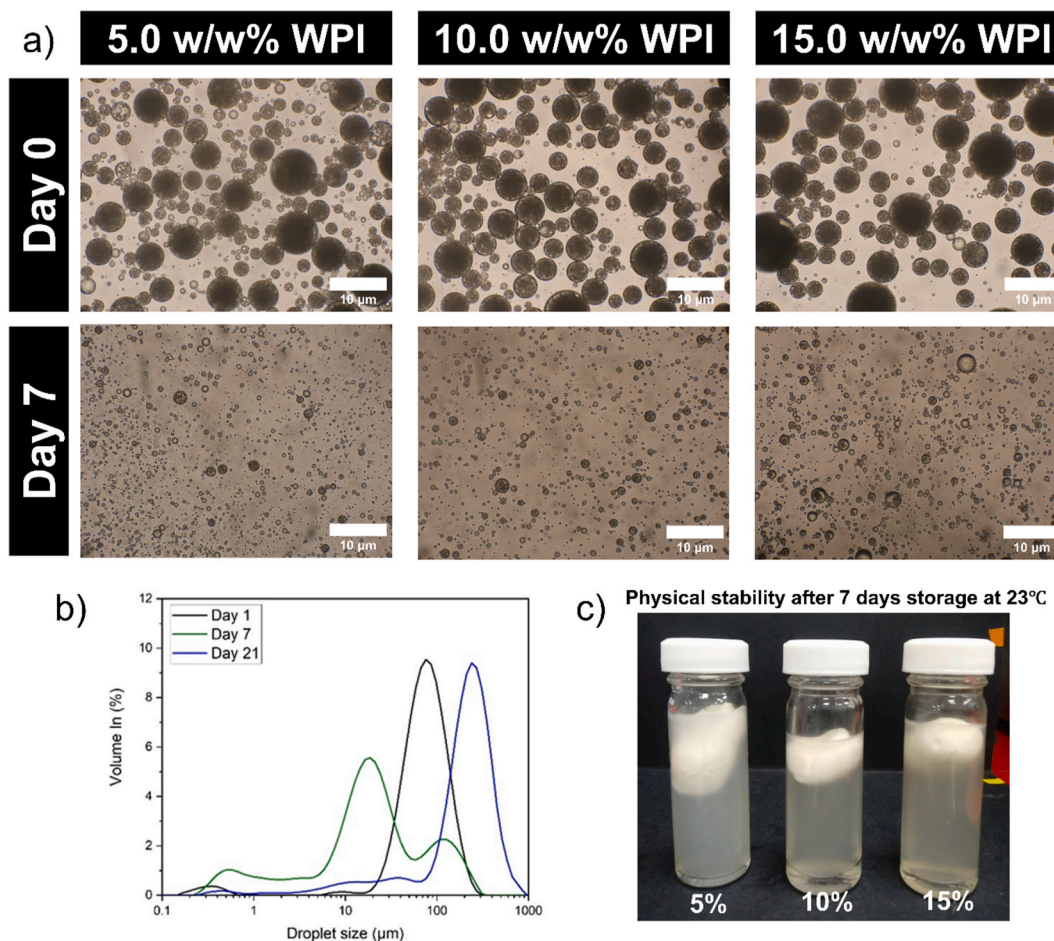


Fig. 2. Microstructural evolution (a) of the $W_1/O/W_2$ double emulsion (DE) (80 v/v% external water) stabilized with different concentrations of WPI (5.0, 10.0 and 15.0 w/w%) of WPI, whilst the W_1/O inner emulsion droplets was stabilized with 10CBolg over a week storage. Changes in droplet size for 5.0 (w/w%) of WPI (b) DE storage over a period of 21 day at $21\ ^\circ\text{C}$. The physical destabilization of the DE emulsions is presented using visual photographs in figure (c). The data reported are the means of three replicates.

centered at an equivalent diameter $<1\ \mu\text{m}$, corresponding to the smaller oil droplets of a W/O single emulsion that might have not formed DE during the homogenization process, and a second peak at higher size (about $76\ \mu\text{m}$ for the droplet size) that corresponds to the DE distribution (Fig. 2b). However, after a week of storage at $21\ ^\circ\text{C}$, the droplet size distribution was shifted to a lower mean size and presented a multimodal distribution (Fig. 2b), which is associated to a significant destabilization process, also observed with drastic loss of DE droplets on day 7 (Fig. 2a). As the crystals tend to reach the equilibrium state (21 days), an opposite trend is observed, as evidenced by an increase in the droplet size distribution with the appearance of a third peak indicative of agglomeration, generated largely by partial coalescence of droplets (Fig. 2b), culminating in the formation of a solid-like cream layer containing the residual encapsulated water post homogenization (Fig. 2c). The three distinct peaks corresponding to small oil droplets, few remained DE droplets, and agglomerates were located at 0.4, 70 and $400\ \mu\text{m}$ droplet diameter, respectively. Due to the instability of the systems (Fig. 2c), the light scattering data should be taken with caution, nevertheless, highly congruent with the visual images (Fig. 2b). The DEs formed a cream layer as illustrated in Fig. 2c. However, this cream layer, once formed, resisted dispersion upon shearing. Noteworthy, the presence of crystals within the internal emulsion might have triggered the destabilization of the DEs, as equivalent DEs (e.g., fractions of oil and water phases) created with non-Pickering system *i.e.* polyglycerol polyricinoleate (PGPR) and whey protein isolate (WPI) remained stable under identical storage conditions (see Supplementary Information, Fig. S2).

The mechanism underlying the destabilization of Pickering/protein-stabilized DE may involve various phenomena occurring at the same time. These include interactions between proteins and crystals, the inherent characteristics of the crystals such as their melting, structural re-arrangement, the SFC and interfacial properties, dimensions of the DE droplets and the encapsulated internal water droplets. Whilst we conducted assessments to characterize macrostructural and microstructural changes and obtained insights into the overall properties of the dispersions, the underlying molecular structures at the interface and their dynamics are beyond the scope of this work. Nelis et al. (2019) reported that fat crystals improve the diffusive stability by reducing permeability of the oil phase, as the formation of crystal networks increase the tortuosity of the diffusive path by the formation of a shell. However, an observation emerged from the evolution of the DE stabilized with 5% WPI storage for 7 days, reveal a shrinking in DE droplet size (Fig. 2b). Potential melting of some crystals at the interface of the internal W/O emulsion droplets during its incorporation to the W_2 phase whilst homogenization, attributed to the temperature increase induced by the shearing forces, cannot be completely ignored.

WPI molecules possess regions that are both hydrophobic and hydrophilic, allowing them to swiftly adhere to the interface between oil and water, forming a viscoelastic interfacial layer. This, in turn, offers structural reinforcement to oil droplets by electrostatic interactions (Cornacchia & Roos, 2011; Sun & Gunasekaran, 2009). Increasing WPI concentration should enhance the WPI adsorption and surface coverage, improving stability of the DE. However, our results suggests that destabilization behavior persisted even at higher concentrations of WPI (15 wt %), with very few DE droplets and complete separation of the W/O emulsion phase from the W_2 phase during storage (Fig. 2c). The droplet size distribution for 10.0 and 15.0 w/w% WPI concentration presented similar trends, characterized by a bimodal distribution with comparable droplet size. Over time, similar increase in droplet size was observed in DEs containing 10–15.0 w/w% WPI as those stabilized with 5.0 w/w% WPI (see Supplementary Information, Fig. S3), ultimately resulting in the loss of the DEs structures, as shown in Fig. 2a. Previous studies have reported a synergistic interaction between proteins and fat crystals at the interface, leading to an increase in interfacial shear viscosity, a phenomenon also influenced by the polymorphic form of the crystals (Ogden & Rosenthal, 1998). However, our experimental

observation shows that WPI offer limited stability to the DE droplets, which might be associated with the variations in oleogel composition (CB + HOSO system) and associated protein interactions used in the study.

Indeed, polarized light microscopy (PLM) in Fig. 3a reveals CBolg crystals-associated partial coalescence in DEs after 2 h of preparation, emphasizing the protrusion of WPI-interfacial membrane by the CBolg crystals. The micrograph shows pairs of droplets joined by CBolg crystals, visible due to their distinctive light emission under polarized light. Piercing of interfacial membranes by fat crystals has been reported in previous literature as a potential destabilization mechanism (Cheng, Kan, Cao, Dudu, & Yan, 2021). These findings prompt inquiries into the destabilization of DE facilitated by CBolg crystals and a combination of crystal characteristics such as the size and orientation geometry within the oil globule, may significantly promote the piercing of crystals through the protein-stabilized oil-water interface (Fredrick, Walstra, & Dewettinck, 2010). This phenomenon induces partial coalescence of the oil DE droplets, eventually resulting in coalescence of the entire system. After a week of storage, the resulting cream consisted primarily of the stable W_1/O emulsion. This can be confirmed by the micrograph taken from the cream, showing that the internal Pickering W_1/O emulsion droplets indeed maintained their integrity during shearing and storage of the DE (see upper micrograph of Fig. 3b). However, the sub nanatant contained only a few remaining DE droplets (see bottom micrograph of Fig. 3b) suggesting droplet break of non-Pickering DEs stabilized by WPI into inner Pickering W_1/O droplets.

Fig. 3c depicts the proposed destabilization mechanism of the DE when using WPI in the external phase. The CBolg crystals located at oil-water interfaces (Fredrick et al., 2010), protrude through the WPI-coated oil-water interface. Upon aging, CBolg crystals become fewer and larger (due Ostwald ripening) and can more easily pierce through the interface and form connections with other DE droplets, as evidenced in the PLM micrograph of Fig. 3a. As the process unfolds, the WPI-interfacial barrier eventually ruptures, leading to the formation of an oil neck that connects two oil droplets through a fat crystal bridge (Fredrick et al., 2010), as depicted in the drawing presented in Fig. 3c. When the globules stay linked, the process is known as partial coalescence, however this might be an intermediate process which will lead to eventual DE coalescence and finally the separation of the DE occurs into a creaming phase containing the W/O emulsion phase, free oil and an aqueous phase containing smaller oil droplets and some small DE droplets (Fig. 3b). Moreover, the size of droplets could exert a significant influence on the drainage of the continuous phase between them, typically preventing droplets collision. This circumstance facilitates further piercing by crystals, ultimately resulting in the destabilization of the DEs. An alternative solution to enhance stability of DE would be to use a Pickering particle, using the same WPI, but subjected to a terminal and breaking process, it possible to create Pickering particles. It was important to understand if conversion of WPI into WPM will resist the piercing of the crystals.

3.2. Characterization of WPM

The heat treatment employed during WPM preparation facilitates the conversion of the parent WPI into covalently crosslinked gels, through the formation of intramolecular disulfide bonds. The following shearing process yields small particles characterized by a narrow monomodal distribution, with a mean equivalent diameter of $100 \pm 0.7\ \text{nm}$ (Fig. 4a). Furthermore, the ζ -potential values of WPM particles are dependent of the protein concentration and can exhibit a range from positive to negative, influenced by the medium's pH. From the experimental results, the ζ -potential of the WPM at pH 7.0 was $-27.7 \pm 0.9\ \text{mV}$ in line with the range reported in previous studies (do Prado Silva et al., 2021; Sarkar et al., 2016). Fig. 4b presents a scanning electron microscopy (SEM) micrograph of a 5.0 (v/v%) WPM microgels suspensions. The image reveals irregular aggregates of WPM particles subsequent to the

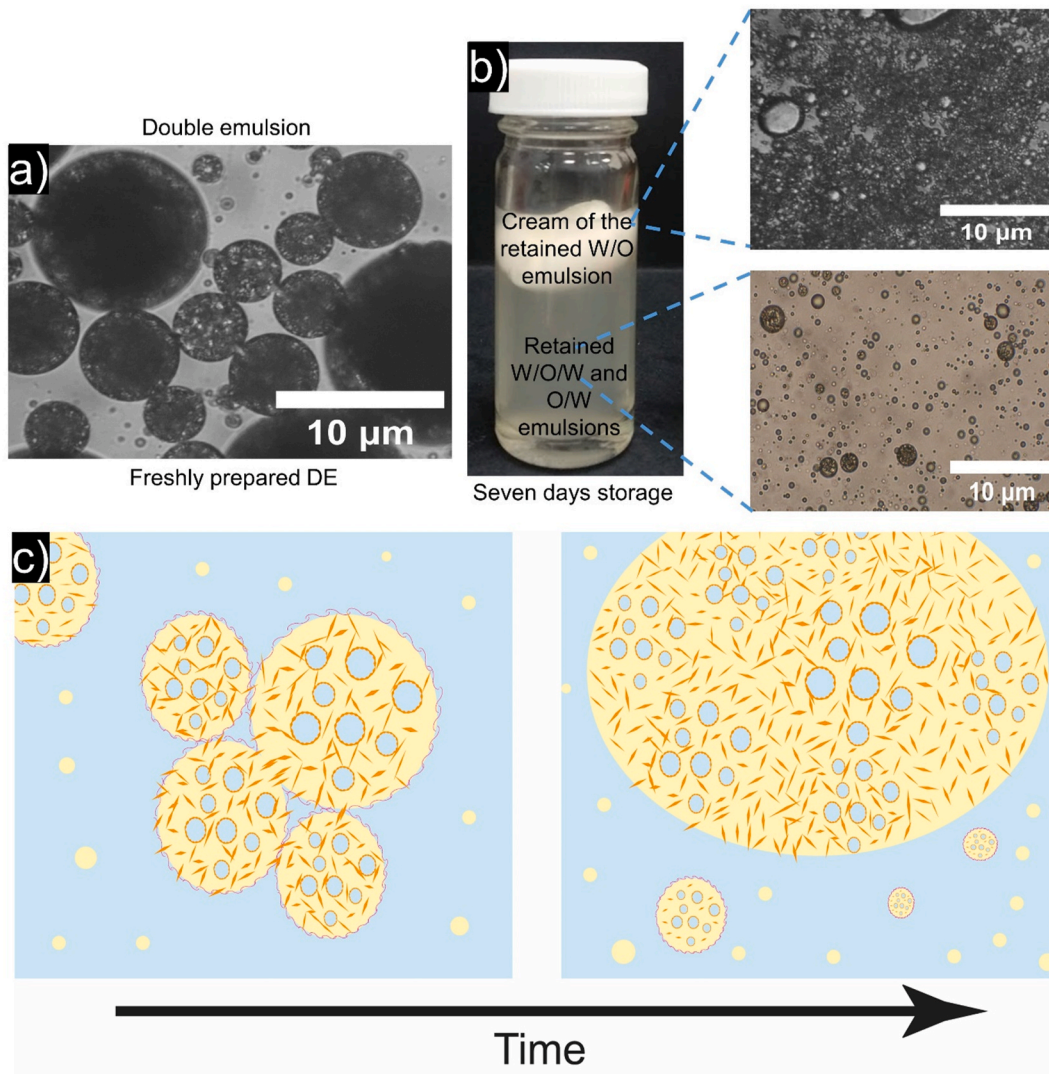


Fig. 3. Polarized light micrographs of a freshly prepared DEs containing WPI as the emulsifier for the external droplet (a), highlighting the protrusion of CBolg crystals within the DE droplets. Visual image showing physical destabilization of the DE (b), with the microstructure of the formed cream layer (top) containing the coalesced DE droplets and breakup into simple W_1/O emulsions and subnatant (bottom) showing remaining DE droplets after 7 days of storage at 21 °C. Schematic representation of the proposed destabilization mechanism (c) of DEs stabilized by CBolg crystals and WPI. The primary W_1/O emulsion was made with 10CBolg.

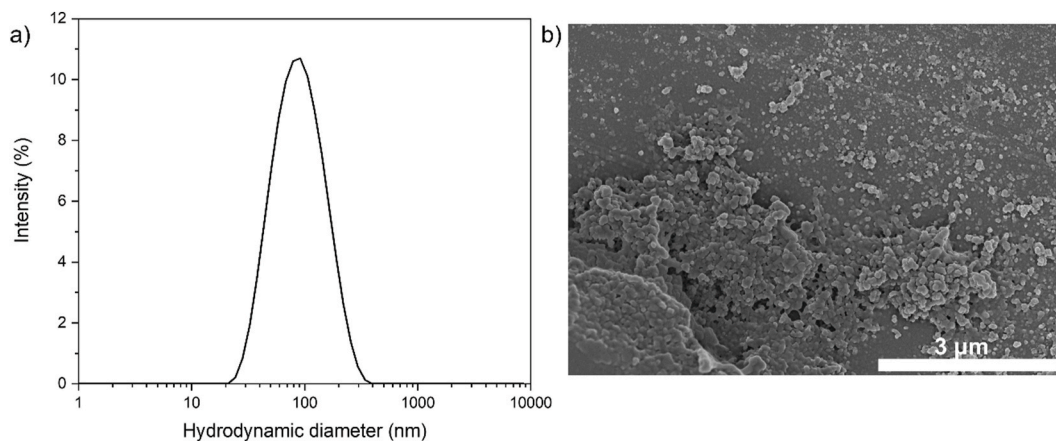


Fig. 4. Mean particle size distribution (a) and SEM image (b) of WPM (5.0 v/v%) dispersion at pH 7.0.

drying process. Despite the irregular shapes observed, WPM particles typically possess a soft nature, facilitating their ability to flatten at the oil-water interface (O/W₂) of the DE. This phenomenon enhances interfacial anchorage, thereby contributing to the overall stability of the emulsion.

In Fig. 5, SAXS data is displayed for nonmicrogelled WPI in solution and the aqueous dispersion of WPM. Both samples were measured at 21 °C and their SAXS curves are superimposed in Fig. 5a. The WPI in solution (green) displays a classical protein scattering curve and the Guinier plot analysis (Fig. 5b) resulted in a radius of gyration, R_g , of 2.19 ± 0.02 nm ($R^2 = 0.99812$), which is in excellent agreement with published literature values of WPI in solution (Li et al., 2021). The scattering curve of the WPM sample has been interpreted along the lines of a Guinier-Porod model (Hammouda, 2010). We note that the particle size of about 100 nm of this WPM dispersion (see DLS results in Fig. 4a) is too large to be observed with SAXS (Fig. 5a). Consequently, both the expected plateau with a $1/q^0$ dependency and the first Guinier region of these particles are not recorded. Nevertheless, the inner nanostructure of the particles, arising from the microgel structure can be confirmed by two different Porod regions with a lower q -dependency of $1/q^{1.8}$ and higher q -dependency of $1/q^{3.5}$. Note, for convenience the exponents are given for a point focus configuration, while the data was recorded with line focus instead (here the exponents are -0.8 and -2.5 , respectively; Fig. 5a). From the first Porod region we conclude that the whey protein gel consist of partially stretched or tangled protein strands (note, a perfectly fully-stretched strand would display an exponent of -1 (Hammouda, 2010)), and from the second Porod region we conclude that along the tangled protein strand coiled or even collapsed protein-chain units are present (note, perfectly globular sub-units would lead to an exponent of -4 (Li et al., 2021)). Summarizing, SAXS data clearly confirms the expected structural differences between WPI and WPM. While WPI exhibits intact proteins in solution, WPM displays a hierarchal arrangement characterized by partially stretched protein strands with smaller sub-units of folded protein portions.

3.3. Dual Pickering stabilization: incorporating WPM to stabilize the external droplets in DEs

The investigation assessed the optimal concentration of WPM needed and the corresponding processing conditions to obtain maximal stability in DEs. To ensure consistency for comparative purposes, the formulation and processing conditions of the primary emulsion were maintained

constant using 10CBolg (10 v/v% CB) throughout all experiments. All the DEs were prepared after 10 min of preparing the primary emulsion, as the development of the CBolg crystal network increase the viscosity of the systems and therefore complicate the formation of the DEs due to the increased viscosity of the W/O emulsion. Key parameters considered for evaluating the stability of dual Pickering-stabilized DEs included the concentration of the secondary stabilizer (WPM) at 3.0 v/v% and 5.0 v/v%, with secondary shear conditions set at 9,400 and 11,000 rpm.

Notably, the incorporation of WPM showed a substantial enhancement in the stability of DEs compared to nonmicrogelled WPI. This improvement was evident as visual structure of the DE droplets remained over the entire four-week storage period (Fig. 6). Upon examination of the optical micrographs, some changes in the structure of the DEs were detected, depending on the WPM concentration. DEs processed with 3.0 v/v% WPM exhibited a notable change at week 1, characterized by a reduction in the number of DE droplets. Higher WPM concentrations (5 v/v%) were more resistant to coalescence, as more DE droplets are maintained over the time. Although the formation of flocs persisted in WPM-stabilized DEs, creaming and most importantly coalescence did not occur (see Supplementary Fig. S4).

Two different concentrations, 3.0 wt% (3WPM) and 5.0 wt% (5WPM), were employed to assess the impact of WPM on stability of dual Pickering stabilized DEs. Light scattering measurements were used to evaluate the stability by examining changes in the volume mean diameter ($D_{[4,3]}$), which provides insights into floc formation. Initially, $D_{[4,3]}$ values shifted from 86 μm to 216 and 192 μm for 3WPM and 5WPM, respectively, after 4 weeks of storage (Fig. 7a). However, two phenomena were observed in the distribution (Fig. 7b and c). Firstly, there was a reduction in the droplet size compared to day 0, similar to the DEs stabilized by WPI (Fig. 2), indicating the loss of internal water. Literature reports that fat crystals confer stability against diffusion, thus no increase in the droplet size should be occurring. However, it is possible that some crystals in the W/O emulsions melted during the second homogenization, allowing the diffusion of the non-encapsulated water. Nevertheless, unlike non-microgelled DEs, the main peak was maintained and a small peak at higher droplet size appeared after 28 days of storage (indicated by the arrow in Fig. 7c and d), signifying the onset of partial coalescence (see Fig. S4 as small flocs on the container wall). A higher degree of floc formation was observed in emulsions with a lower WPM concentration. These findings suggest that, despite the more effective surface coverage of WPM particles, there exists a minimum concentration below which optimal stability could not be

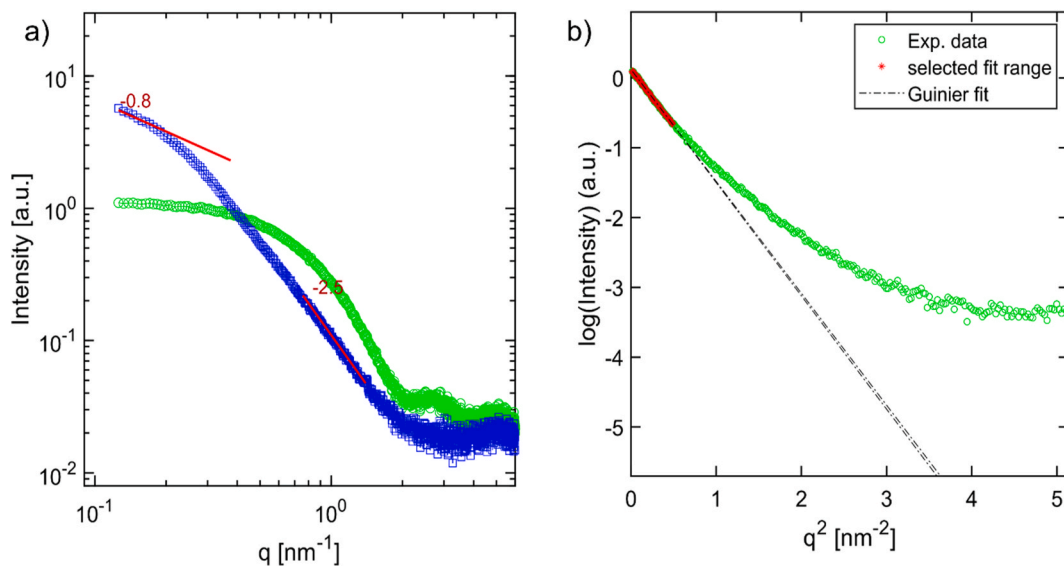


Fig. 5. SAXS curves (a) of 5.0 (v/v%) WPI in solution (green) and 5.0 (v/v%) WPM dispersion (blue) with Guinier plot analysis (b) of WPI. Two Porod slope regions are identified for the WPM sample in (a).

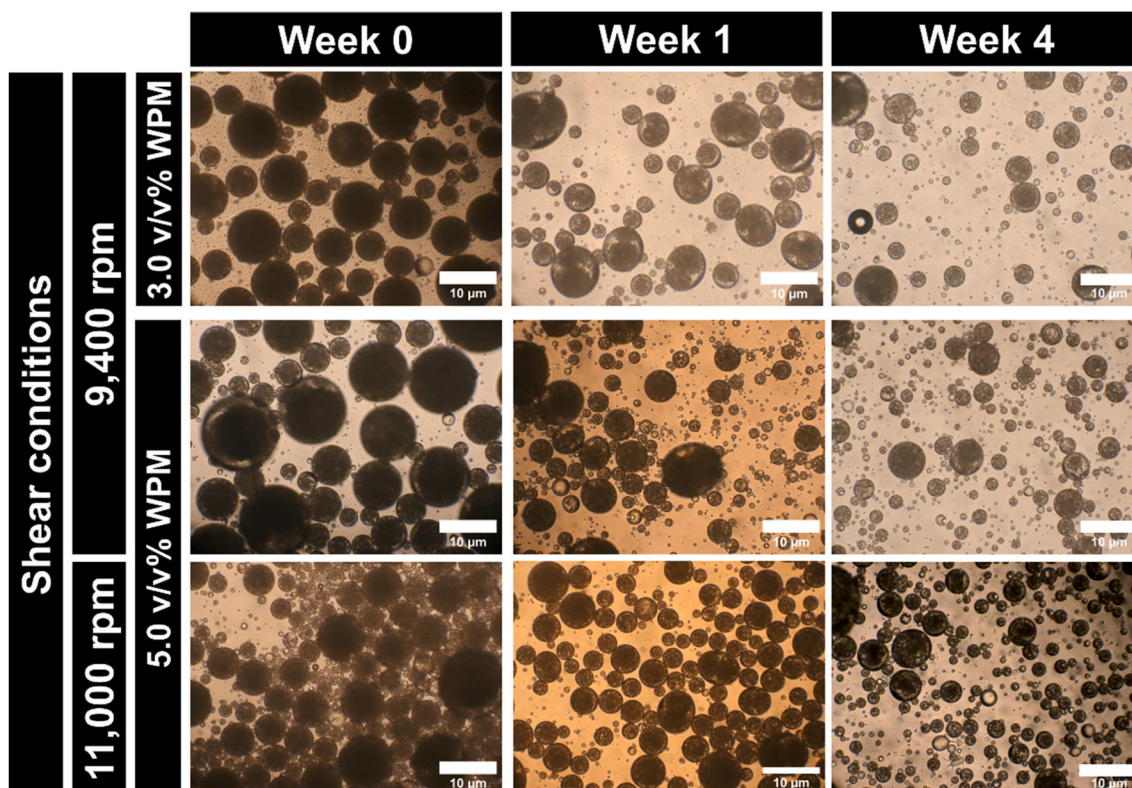


Fig. 6. Effect of the WPM concentration and shear conditions in the microstructure of the DE. The optical micrographs depict the evolution of the droplets when they are stored for 4 weeks at 21 °C. DE prepared with different WPM concentration (3.0 or 5.0 v/v%) were homogenized at 9,400 rpm. For the 5.0 (v/v%) WPM concentration, the homogenization was also carried out at 11,000 rpm. A 10CBolg was used as Pickering particles for the primary emulsion.

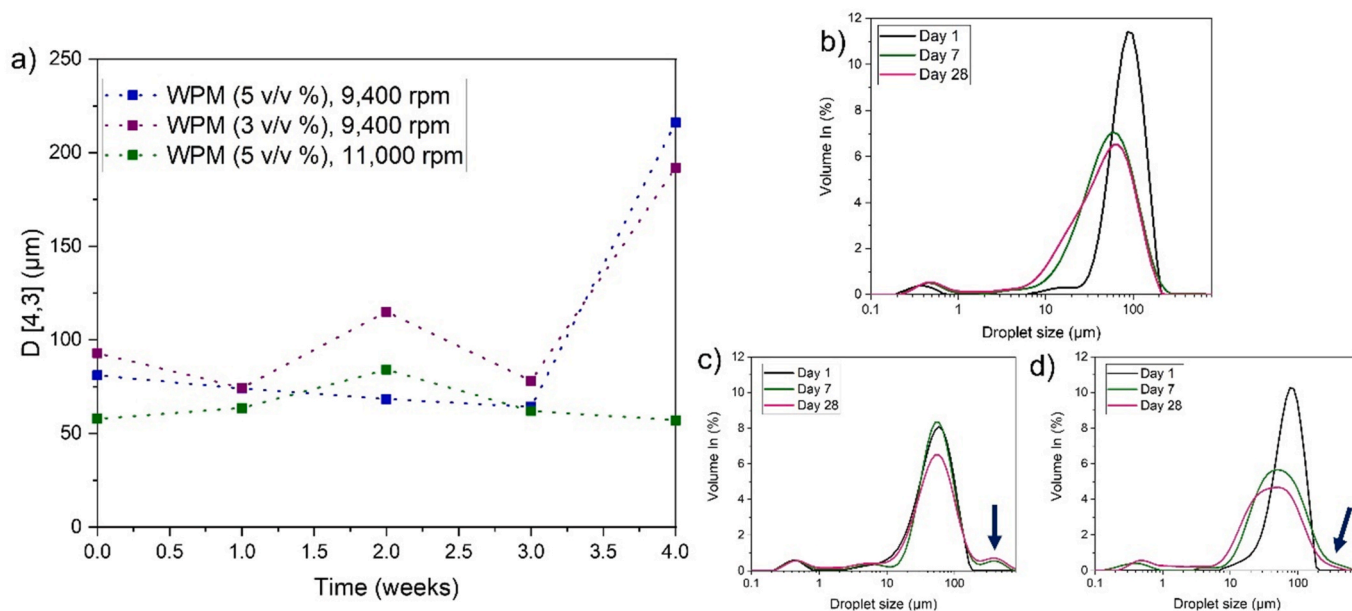


Fig. 7. Mean droplet size ($D_{[4,3]}$) (a) evolution of DEs as a function of time with distribution of DEs stabilized by 5.0 (v/v%) WPM at 11,000 rpm (b) and at 9,400 rpm (c); whilst (d) shows DEs stabilized by 3.0 (v/v%) WPM at 9,400 rpm.

achieved. Consequently, higher concentration of WPM was needed to prevent droplet coalescence by maintaining a sufficient spatial separation between the DE droplets.

The increase of homogenization speed from 9,400 to 11,000 rpm in the second emulsification step, revealed a visible improvement in the stability of the dual Pickering-stabilized DEs. This enhancement was

evident in the DE microstructure, wherein more DE droplets were formed and persisted over time (Fig. 7b), and the formation of flocs was barely noticeable (see Supplementary Information, Fig. S4). Simultaneously, the average droplet size exhibited a slight reduction, yielding values of 53.6 µm compared with the DEs formed at lower homogenization velocity (9,400 rpm) with 5WPM. Notably, an examination of the

$D_{[4,3]}$ values revealed a progressive increase of the size of DE droplets over time, for the sample produced at 9,400 rpm (Fig. 7), whereas DEs processed at 11,000 rpm maintained the same size distribution over the four weeks, possibly due to the smaller average droplet size produced with these processing conditions. In addition, the sample did not show a third peak visible as the DE with lower shear rate.

The viscoelastic monolayer of WPI proteins at the oil-water interface (Pelán, Watts, Campbell, & Lips, 1997), was found to lack the required strength to withstand the protrusion of CBolg crystals, resulting in coalescence of the DE droplets. In contrast, WPM provided a stronger steric barrier against coalescence (Akgonullu et al., 2023; Dickinson, 2015). The hierarchical structure of WPM particles, observed in the SAXS results is believed to contribute to the enhanced stability of the DE against CBolg crystal piercing, as it restricts the piercing by the CBolg crystals. We hypothesize that these distinctive properties contribute to the superior stability observed when utilizing WPM in DEs as compared to WPI. To gain a deeper understanding of the higher stability, we conducted observations of the internal structure at the interface of the DE oil droplets, which will be discussed in the following section.

3.4. Multiscale microstructure of the dual Pickering-stabilized DEs

CLSM facilitates the differentiation of structural compositions within the samples by fluorescing each phase with specific dyes. This method not only allows for the discerning different phases within the DE, but it also enables the identification of Pickering particles at the interfaces. Observations were focused on DEs stabilized by 5.0 v/v% WPM at 11,000 rpm, as this was the most stable system, utilizing CLSM and cryo-SEM. Fig. 8a depicts the microstructure of the DEs using the combination of the three dyes, revealing the presence of a DE. The micrograph shows NR-stained red oil droplets containing darkened water droplets, which had the edge colored in green, confirming the presence of CBolg crystals fluoresced using NB. However, WPM particles at the interface of the oil droplets could not be observed. The high concentration of the WPM particles in the bulk water phase (W_2) did not allow clear observation of WPM at interfaces since all the continuous phase appeared bright green. However, subsequent dilution (1:1) of this continuous phase enabled the visualization of FG-stained WPM surrounding oil droplets, as depicted in green in Fig. 8b.

A more detailed morphological examination of the internal microstructure of the DE was achieved through cryo-SEM micrographs. Fig. 9a presents a cross-sectional view revealing spherical indentations as well

as completed droplets on the fractured surface, indicative of internal water droplets (W_1) within the analyzed oil droplet. Zooming on one of the inner water droplets (Fig. 9b) revealed the presence of surface layers of CBolg crystal along with CBolg crystals dispersed in the bulk phase. This observations aligns with previous findings on the stabilization mechanism of CBolg crystals (Tenorio-Garcia et al., 2023). Observing at the oil-water interface, we could see a monolayer of WPM, as surface of hemi-spherical bumps (Fig. 9c), commonly referred to as a “fried-egg” morphology at the interface (Camerin et al., 2019). These comprehensive multiscale observations offer valuable insights into the intricate microstructural details and spatial distribution of the two Pickering particles within the examined dual Pickering-stabilized DEs.

4. Conclusions

This study demonstrated the efficacy of CBolg crystals and WPM as stabilizers in dual Pickering stabilized DEs, emphasizing the significant role of Pickering particles in mitigating coalescence phenomena. The CBolg crystals, employed as Pickering particles in the primary emulsion, conferred high stability to the W_1/O emulsions, which could resist the secondary homogenization process in case of DEs stabilized by non-microgelled WPI. However, CBolg crystals can promote coalescence during storage as they protrude out of their DE droplet and create connections with other droplets. Despite the presence of a WPI monolayer at the oil-water interface, WPI fails to prevent the protrusion of CBolg crystals, resulting in DE instability. In contrast, WPM offered a more resistant steric barrier against CBolg crystal protrusion and coalescence, with superior stability of WPM-stabilized DEs over a month as compared to WPI-stabilized ones that showed coalescence in a week's storage. Additionally, changing homogenization shear may also lead to further improvement in DE stability. The results of this work highlight the efficacy of WPM particles in stabilizing DEs and underscore the importance of optimal WPM concentration and processing conditions in achieving and maintaining stability. A key limitation of this study is lack of measurement of the size of inner droplets and how changing size of those droplets may influence stability of the DEs, which needs investigation in future studies. In summary, the findings from this study contribute to the understanding of the dual Pickering stabilization mechanisms in DEs, providing valuable insights for the design and formulation of stable emulsion, particularly in application within the food industry for co-delivery of bioactive and fat reduction applications.

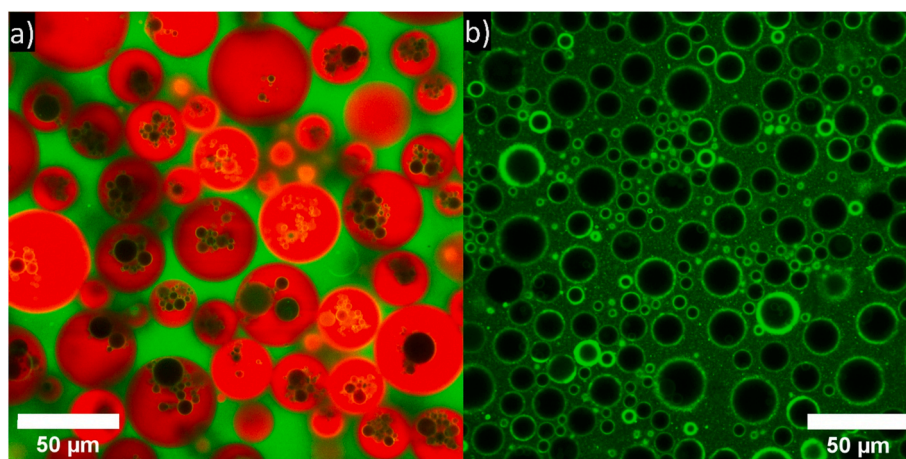


Fig. 8. Confocal image of DE (a) stabilized with 5.0 (v/v%) WPM. The internal structure of the DE are fluoresced using Fast Green, Nile Blue and Nile Red staining WPM, CBolg crystals and fat droplets, respectively. Microstructure of a DE with a 1:1 dilution, only using Fast Green excitation (b) showing the WPM interfacial layer at surface of the DE droplet. The DEs were prepared at 11,000 rpm and stored at 21 °C, before being dyed for observation. Adjusting the focus led to the disappearance of some internal water droplets from the oil droplets, this phenomenon was primarily influenced by changes in the focal plane rather than the presence of simple emulsions.

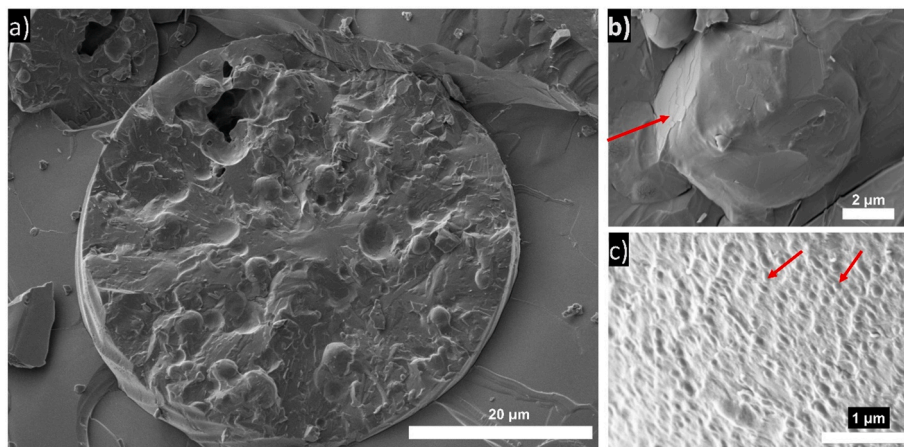


Fig. 9. Cryogenic scanning electron microscopy (Cryo-SEM) images (a) of the DE emulsion droplet morphology and the zoom of the internal water droplets stabilized by CBoI crystals (marked by the red arrow) (b) and a zoom of the oil droplet interface (c) where WPM particles are shown by red arrows.

CRediT authorship contribution statement

Elizabeth Tenorio-Garcia: Writing – review & editing, Writing – original draft, Methodology, Investigation, Funding acquisition, Formal analysis, Data curation, Conceptualization. **Michael Rappolt:** Writing – review & editing, Supervision, Methodology, Data curation, Conceptualization. **Amin Sadeghpour:** Writing – review & editing, Methodology, Data curation, Conceptualization. **Elena Simone:** Writing – review & editing, Supervision. **Anwasha Sarkar:** Writing – review & editing, Supervision, Project administration, Conceptualization.

Declaration of competing interest

No conflicts of interests.

Data availability

Data will be made available on request.

Acknowledgements

ET-G acknowledges financial support from the Mexican National Council of Science and Technology (CONACyT) for the award of an Academic Scholarship for her PhD studies. ES has received funding for this collaboration from the European Research Council (ERC) under the European Union's Horizon 2020 research and innovation program (grant agreement No 949229).

Appendix A. Supplementary data

Supplementary data to this article can be found online at <https://doi.org/10.1016/j.foodhyd.2024.110327>.

References

- Akgonullu, D. Z., Murray, B. S., Connell, S. D., Fang, Y., Linter, B., & Sarkar, A. (2023). Synthetic and biopolymeric microgels: Review of similarities and difference in behaviour in bulk phases and at interfaces. *Advances in Colloid and Interface Science*, 320, Article 102983.
- Binks, B. P. (2002). Particles as surfactants—similarities and differences. *Current Opinion in Colloid & Interface Science*, 7(1), 21–41.
- Boode, K., & Walstra, P. (1993). Partial coalescence in oil-in-water emulsions 1. Nature of the aggregation. *Colloids and Surfaces A: Physicochemical and Engineering Aspects*, 81, 121–137.
- Boode, K., Walstra, P., & de Groot-Mostert, A. E. A. (1993). Partial coalescence in oil-in-water emulsions 2. Influence of the properties of the fat. *Colloids and Surfaces A: Physicochemical and Engineering Aspects*, 81, 139–151.

- Boumelhem, B. B., Pilgrim, C., Zwicker, V. E., Kolanowski, J. L., Yeo, J. H., Jolliffe, K. A., et al. (2021). Intracellular flow cytometric lipid analysis – a multiparametric system to assess distinct lipid classes in live cells. *Journal of Cell Science*, 135(5).
- Camerin, F., Fernández-Rodríguez, M.Á., Rovigatti, L., Antonopoulou, M.-N., Gnan, N., Ninarello, A., et al. (2019). Microgels adsorbed at liquid–liquid interfaces: A joint numerical and experimental study. *ACS Nano*, 13(4), 4548–4559.
- Chen, S., Du, Y., Zhang, H., Wang, Q., Gong, Y., Chang, R., et al. (2022). The lipid digestion behavior of oil-in-water Pickering emulsions stabilized by whey protein microgels of various rigidities. *Food Hydrocolloids*, 130, Article 107735.
- Cheng, J., Kan, Q., Cao, J., Dudu, O. E., & Yan, T. (2021). Interfacial compositions of fat globules modulate coconut oil crystallization behavior and stability of whipped-frozen emulsions. *Food Hydrocolloids*, 114, Article 106580.
- Cornacchia, L., & Roos, Y. H. (2011). Lipid and water crystallization in protein-stabilised oil-in-water emulsions. *Food Hydrocolloids*, 25(7), 1726–1736.
- Cui, C., Zeng, C., Wang, C., & Zhang, L. (2017). Complex emulsions by extracting water from homogeneous solutions comprised of aqueous three-phase systems. *Langmuir*, 33(44), 12670–12680.
- Dekker, R. I., Velandia, S. F., Kibbelaar, H. V. M., Morcy, A., Sadtler, V., Roques-Carnes, T., et al. (2023). Is there a difference between surfactant-stabilised and Pickering emulsions? *Soft Matter*, 19(10), 1941–1951.
- Destribats, M., Rouvet, M., Gehin-Delval, C., Schmitt, C., & Binks, B. P. (2014). Emulsions stabilised by whey protein microgel particles: Towards food-grade pickering emulsions. *Soft Matter*, 10(36), 6941–6954.
- Dickinson, E. (2015). Microgels — an alternative colloidal ingredient for stabilization of food emulsions. *Trends in Food Science & Technology*, 43(2), 178–188.
- do Prado Silva, J. T., Benetti, J. V. M., Alexandrino, T. T. d. B., Assis, O. B. G., de Ruiter, J., Schroën, K., et al. (2021). Whey protein isolate microgel properties tuned by crosslinking with organic acids to achieve stabilization of pickering emulsions, 10 p. 1296), 6.
- Fredrick, E., Walstra, P., & Dewettinck, K. (2010). Factors governing partial coalescence in oil-in-water emulsions. *Advances in Colloid and Interface Science*, 153(1–2), 30–42.
- Ghosh, S., & Rousseau, D. (2011). Fat crystals and water-in-oil emulsion stability. *Current Opinion in Colloid & Interface Science*, 16(5), 421–431.
- Ghosh, S., Tran, T., & Rousseau, D. (2011). Comparison of Pickering and network stabilization in water-in-oil emulsions. *Langmuir*, 27(11), 6589–6597.
- Glatter, O., & Kratky, O. (1982). In O. Glatter, & O. Kratky (Eds.), *Small angle X-ray scattering*. London: Academic Press.
- Goibier, L., Pillement, C., Monteil, J., Faure, C., & Leal-Calderon, F. (2019). Emulsification of non-aqueous foams stabilized by fat crystals: Towards novel air-in-oil-in-water food colloids. *Food Chemistry*, 293, 49–56.
- Goibier, L., Pillement, C., Monteil, J., Faure, C., & Leal-Calderon, F. (2020). Preparation of multiple water-in-oil-in-water emulsions without any added oil-soluble surfactant. *Colloids and Surfaces A: Physicochemical and Engineering Aspects*, 590, Article 124492.
- Gould, J., Garcia-Garcia, G., & Wolf, B. (2016). Pickering particles prepared from food waste. 9(9), 791.
- Guan, X., Li, Y., Jiang, H., Tse, Y.-L. S., & Ngai, T. (2023). Temperature-responsive pickering double emulsions stabilized by binary microgels. n/a(n/a), e202300587.
- Guinier, A., & Fournet, G. (1955). *Small-angle scattering of X-rays*. Wiley.
- Hammouda, B. (2010). *A new Guinier-Porod model*, 43 pp. 716–719.
- Herrera, M. L., & Hartel, R. W. (2001). Lipid crystal characterization. *Current Protocols in Food Analytical Chemistry*, 00(1), D3.2.1–D3.2.6.
- Herzi, S., & Essafi, W. (2019). Crystallizable W/O/W double emulsions made with milk fat: Formulation, stability and release properties. *Food Research International*, 116, 145–156.
- Jiang, H., Zhang, T., Smits, J., Huang, X. N., Maas, M., Yin, S. W., et al. (2021). Edible high internal phase Pickering emulsion with double-emulsion morphology. *Food Hydrocolloids*, 111.
- Johansson, D., Bergenståhl, B., & Lundgren, E. (1995). Wetting of fat crystals by triglyceride oil and water. 1. The effect of additives. *Journal of the American Oil Chemists' Society*, 72(8), 921–931.

- Karefyllakis, D., Jan van der Goot, A., & Nikiforidis, C. V. (2019). The behaviour of sunflower oleosomes at the interfaces. *Soft Matter*, 15(23), 4639–4646.
- Lan, M., Song, Y., Ou, S., Zheng, J., Huang, C., Wang, Y., et al. (2020). Water-in-Oil pickering emulsions stabilized solely by water-dispersible phytosterol particles. *Langmuir*, 36(49), 14991–14998.
- Li, J., Yang, Z., Lin, X., Wu, S., Li, G., Li, N., et al. (2021). In-flow SAXS investigation of whey protein isolate hydrolyzed by bromelain. *Colloids and Surfaces A: Physicochemical and Engineering Aspects*, 631, Article 127662.
- Lin, X. Y., Li, S. N., Yin, J. H., Chang, F. D., Wang, C., He, X. W., et al. (2020). Anthocyanin-loaded double pickering emulsion stabilized by octenylsuccinate quinoa starch: Preparation, stability and in vitro gastrointestinal digestion. *International Journal of Biological Macromolecules*, 152, 1233–1241.
- Liu, J., Kharat, M., Tan, Y., Zhou, H., Mundo, J. L. M., & McClements, D. J. (2020). Impact of fat crystallization on the resistance of W/O/W emulsions to osmotic stress: Potential for temperature-triggered release. *Food Research International*, 134.
- Loffredi, E., & Alamprese, C. (2023). Digestion fate and food applications of emulsions as delivery systems for bioactive compounds: Challenges and perspectives. *Food Reviews International*, 1–25.
- Metilli, L., Lazidis, A., Francis, M., Marty-Terrade, S., Ray, J., & Simone, E. (2021). The effect of crystallization conditions on the structural properties of oleofoams made of cocoa butter crystals and high oleic sunflower oil. *Crystal Growth & Design*, 21(3), 1562–1575.
- Nelis, V., Declerck, A., Vermeir, L., Balcaen, M., Dewettinck, K., & Van der Meer, P. (2019). Fat crystals: A tool to inhibit molecular transport in W/O/W double emulsions. *Magnetic Resonance in Chemistry*, 57(9), 707–718.
- Nollet, M., Laurichesse, E., Besse, S., Soubabère, O., & Schmitt, V. (2018). Determination of formulation conditions allowing double emulsions stabilized by PGPR and sodium caseinate to be used as capsules. *Langmuir*, 34(8), 2823–2833.
- Norton, J. E., Fryer, P. J., Parkinson, J., & Cox, P. W. (2009). Development and characterisation of tempered cocoa butter emulsions containing up to 60% water. *Journal of Food Engineering*, 95(1), 172–178.
- Ogden, L. G., & Rosenthal, A. J. (1998). Interactions between fat crystal networks and sodium caseinate at the sunflower oil-water interface. *Journal of the American Oil Chemists' Society*, 75(12), 1–7.
- Pelan, B. M. C., Watts, K. M., Campbell, I. J., & Lips, A. (1997). The stability of aerated milk protein emulsions in the presence of small molecule surfactants. *Journal of Dairy Science*, 80(10), 2631–2638.
- Reinke, S. K., Hauf, K., Vieira, J., Heinrich, S., & Palzer, S. (2015). Changes in contact angle providing evidence for surface alteration in multi-component solid foods. *Journal of Physics D: Applied Physics*, 48(46), Article 464001.
- Sarkar, A., & Dickinson, E. (2020). Sustainable food-grade Pickering emulsions stabilized by plant-based particles. *Current Opinion in Colloid & Interface Science*, 49, 69–81.
- Sarkar, A., Kanti, F., Gulotta, A., Murray, B. S., & Zhang, S. (2017). Aqueous lubrication, structure and rheological properties of whey protein microgel particles. *Langmuir*, 33(51), 14699–14708.
- Sarkar, A., Murray, B., Holmes, M., Ettelaie, R., Abdalla, A., & Yang, X. (2016). In vitro digestion of pickering emulsions stabilized by soft whey protein microgel particles: Influence of thermal treatment. *Soft Matter*, 12(15), 3558–3569.
- Schuch, A., Kohler, K., & Schuchmann, H. P. (2013). Differential scanning calorimetry (DSC) in multiple W/O/W emulsions A method to characterize the stability of inner droplets. *Journal of Thermal Analysis and Calorimetry*, 111(3), 1881–1890.
- Spyropoulos, F., Duffus, L. J., Smith, P., & Norton, I. T. (2019). Impact of Pickering Intervention on the stability of W-1/O/W-2 double emulsions of relevance to foods. *Langmuir*, 35(47), 15137–15150.
- Sun, C., & Gunasekaran, S. (2009). Effects of protein concentration and oil-phase volume fraction on the stability and rheology of menhaden oil-in-water emulsions stabilized by whey protein isolate with xanthan gum. *Food Hydrocolloids*, 23(1), 165–174.
- Tenorio-García, E., Araiza-Calahorra, A., Rappolt, M., Simone, E., & Sarkar, A. (2023). Pickering water-in-oil emulsions stabilized solely by fat crystals. *Advanced Materials Interfaces*, 10(31), Article 2300190.
- Tenorio-García, E., Araiza-Calahorra, A., Simone, E., & Sarkar, A. (2022). Recent advances in design and stability of double emulsions: Trends in Pickering stabilization. *Food Hydrocolloids*, 128, Article 107601.
- Wang, Q., Hu, C., Zoghbi, A., Huang, J., & Xia, Q. (2017). Oil-in-oil-in-water pre-double emulsions stabilized by nonionic surfactants and silica particles: A new approach for topical application of rutin. *Colloids and Surfaces A: Physicochemical and Engineering Aspects*, 522, 399–407.
- Wu, J., Shi, M., Li, W., Zhao, L., Wang, Z., Yan, X., et al. (2015). Pickering emulsions stabilized by whey protein nanoparticles prepared by thermal cross-linking. *Colloids and Surfaces B: Biointerfaces*, 127, 96–104.
- Xiao, J., Lu, X. X., & Huang, Q. R. (2017). Double emulsion derived from kafirin nanoparticles stabilized Pickering emulsion: Fabrication, microstructure, stability and in vitro digestion profile. *Food Hydrocolloids*, 62, 230–238.
- Zembyla, M., Lazidis, A., Murray, B. S., & Sarkar, A. (2019). Water-in-oil Pickering emulsions stabilized by synergistic particle-particle interactions. *Langmuir*, 35(40), 13078–13089.
- Zembyla, M., Lazidis, A., Murray, B. S., & Sarkar, A. (2020). Stability of water-in-oil emulsions co-stabilized by polyphenol crystal-protein complexes as a function of shear rate and temperature. *Journal of Food Engineering*, 281, Article 109991.
- Zembyla, M., Murray, B. S., Radford, S. J., & Sarkar, A. (2019). Water-in-oil Pickering emulsions stabilized by an interfacial complex of water-insoluble polyphenol crystals and protein. *Journal of Colloid and Interface Science*, 548, 88–99.
- Zhai, K., Pei, X., Wang, C., Deng, Y., Tan, Y., Bai, Y., et al. (2019). Water-in-oil Pickering emulsion polymerization of N-isopropyl acrylamide using starch-based nanoparticles as emulsifier. *International Journal of Biological Macromolecules*, 131, 1032–1037.
- Zhang, S., Holmes, M., Ettelaie, R., & Sarkar, A. (2020). Pea protein microgel particles as Pickering stabilisers of oil-in-water emulsions: Responsiveness to pH and ionic strength. *Food Hydrocolloids*, 102, Article 105583.